A comparison of five optical surface topography measurement methods

MARJA METTÄNEN[1] and ULRICH HIRN[2]

[1] Tampere University of Technology, Korkeakoulunkatu 3, 33720 Tampere, Finland, marja.mettanen@tut.fi

[2] Graz University of Technology, Inffeldgasse 23, 8010 Graz, Austria, ulrich.hirn@tugraz.at

ABSTRACT

The results of optical surface topography measurement techniques have been questioned in the past because of possible measurement artifacts due to light penetration into the paper. We compared the topography measurement results from five optical techniques: laser profilometry, shape-from-focus, stripe projection, chromatic sensing and photometric stereo. These techniques were tested on coated and uncoated papers with a PPS roughness range from 0.7 µm to 7.7 µm. We made the measurement results directly comparable by measuring exactly the same regions on the paper samples and registering the resulting topography maps. We then calculated the point-wise Pearson correlation between the maps at different wavelength bands to obtain quantitative values for the similarity of the measurement results at different structure sizes. The correspondences between the measured topography maps were also examined through multivariate linear regression and roughness indices evaluated at two different structure sizes.

For rougher grades like office paper or sack paper the topography measurements from the five measurement techniques showed corresponding results. For a moderately smooth LWC paper the measured topographies agreed to some degree and for smooth SC and WFC papers the agreement was poor. From the available data it is impossible to tell which of the measurement techniques delivers the true surface topography of smooth papers.

***Application:** Surface topography measurements from different optical techniques deliver largely different results for smooth paper grades. For rough papers, however, the results match quite well.*

Topography of paper is a highly relevant quality parameter. Paper roughness has been reported to be associated with low print quality. This has been found for flexo printability of packaging papers [1, 2]. It is also the case for newsprint grades printed with offset [3] and rotogravure [4]. For coated papers surface roughness has also been reported to be related to offset print quality [5], even for wood free coated paper [6], the highest quality grade for printing paper.

Measuring paper surface topography optically has several advantages over the older technique of mechanical, stylus based, measurement. First of all, there has been concern that the stylus is deforming the paper surface during the measurement, thus not capturing its true shape. Second, the stylus based topography measurements do not always deliver a true image of the surface; the result heavily depends on the shape and size of the stylus tip. Small, sharp tips give better image detail, however small tips lead to a high local pressure which deforms the paper up to the degree of scratching the surface. Finally, optical measurement methods are usually faster than mechanical methods. However, there is a

serious drawback in optical topography measurements applied to paper surface. Paper fibers are transparent, and therefore light approaching the paper surface is to a large extent not reflected on the surface but it penetrates into the bulk. That questions the ability of optical topography measurements to actually locate the true surface of the paper. It is very likely that light reflected from within the paper bulk influences the measurement result.

Comparison of different paper surface topography measurement techniques has been reported in several publications [7]. Wågberg and coworkers compared a laser profilometry method with a stylus based method [8, 9]. They found measurement artifacts as high as several micrometers for the laser profilometry measurement of paper surface. Furthermore, the surface profile was exaggerated by the laser profilometer, in particular on surfaces having small but steep local slopes. Kuparinen measured the surface topography of paper and paperboard samples with two laser profilometers and found significant, direction-dependent, differences between the topography maps produced by the two devices, particularly at short wavelengths; see Fig. 7.4 in Kuparinen's thesis [10]. Mettänen and coworkers compared photometric stereo based topography measurements to topography maps estimated from X-ray micro-tomography data of paper using registered measurements and 2D coherence [11]. The topography data correlated well at longer wavelengths between 100 µm up to a few millimeters, however on smaller length scales, e.g. around the size of fiber width did not. Lechthaler and Bauer compared laser profilometry, shape-from-focus and mechanical stylus measurements using registered topography data and point-wise correlation of the local topography values [12]. In their investigation, the mechanically measured surface topography had higher variation than the optically measured. The overall correlation between the measurements, rescaled to a dot size of 0.2 x 0.2 mm², was not very high, between $R^2 = 0.4$ and $R^2 = 0.5$. Finally, Lähdekorpi et al. compared three optical paper surface topography measurement techniques, photometric stereo, laser profilometry and white light interferometry. The differences between these methods were considerable, compare Fig. 2 in their work [13].

The current work presents a comparison of surface topography measurements made with five different optical techniques and using a range of clearly different paper grades from kraft sack paper to wood free coated (WFC) paper. We analyzed the similarity of the measuremens quantitatively using spatial registration of the topography data followed by point-wise correlation and regression. The following section will describe the materials and methods in detail. After that, we introduce the results of the study, and finally present conclusions.

EXPERIMENTAL

We applied five different optical techniques for paper surface topography measurement: laser profilometry, shape-from-focus, stripe projection, chromatic sensing and photometric stereo. In this section we first give a short overview on these surface measurement techniques. Then we describe the analyzed papers and the sample preparation. Finally we describe the methods to quantify the similarity of the topography measurements.

Shape from focus

The first measurement technique we applied is shape-from-focus (SFF). We used an Alicona Infinite Focus G3 instrument. It is described in detail by Danzl and coworkers [14], and a sketch of the technique is shown in **Fig. 1**. The paper surface (6) is imaged by a microscopy-like imaging system. The path of the light starts at a white light source (3), and passes illumination optics (2,9,11), a semitransparent mirror (4), and an objective lens (5). From there the light falls on the paper and is partly reflected into the objective (5), from where it proceeds through imaging optics to a CCD camera sensor array (1). The key feature of the optical system is that it has a very narrow depth of focus. The focal position of the imaging system is varied vertically, which results in images where different

regions of the surface are sharply imaged. The shape of the surface is inferred from a set of surface images (7) captured at different focal positions. For each point on the surface there is one image where it is sharply focused (8). Knowing the focal position of the image, the height coordinate of each point can be calculated.

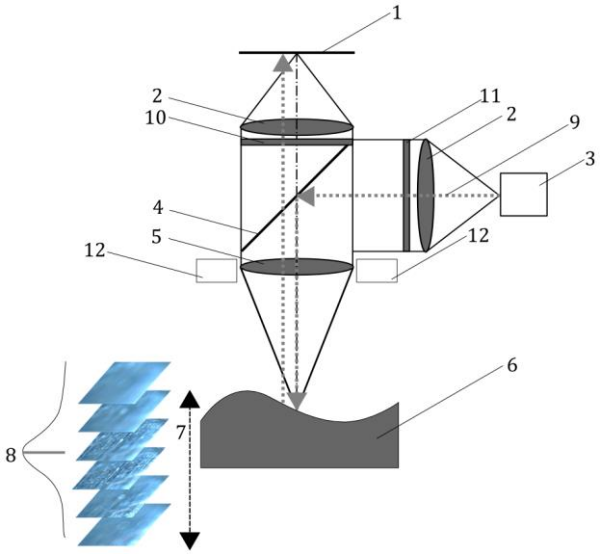

1. Measurement principle for shape-from-focus [14]. See text for the description of the numbering. The ring light (12) was not used in this study.

Shape-from-focus has gained some popularity in paper analysis because together with the paper surface topography map it delivers an optical color image of the paper surface [15]. The optical image can be shown as a texture warped onto the paper surface topography. This enables convenient analysis of e.g. topography related print defects like missing printing ink in paper surface dents.

Chromatic sensor

A measurement technique with no moving mechanical parts is the chromatic sensor. We used a chromatic white light sensor on an FRT Micro Glider instrument. Chromatic white light sensors exploit *chromatic aberration*, the fact that for a given lens the focal position is dependent on the wavelength of light. The principle is exemplified in **Fig. 2**. The measurement device brings light from a white light source through fiber optics to the sensor head where it is projected to the surface. The light is reflected from the surface, collected in the optics and transmitted back into the optical fiber. This reflected light is finally coupled out of the optical fiber and its spectrum is analyzed in a spectrometer. The focal position of the different wavelength components varies in z-directional position, thus the intensity of the reflected light is maximal at the wavelength where the reflecting surface is exactly in focal distance to the lens. The maximum in the reflected light spectrum thus indicates the wavelength in focus and therefrom the distance between the surface and the sensor head. This type of analysis is very fast, however, the speed is lost to some extent because for a 2D measurement the sensor has to be moved laterally for point-wise scanning of the measurement area.

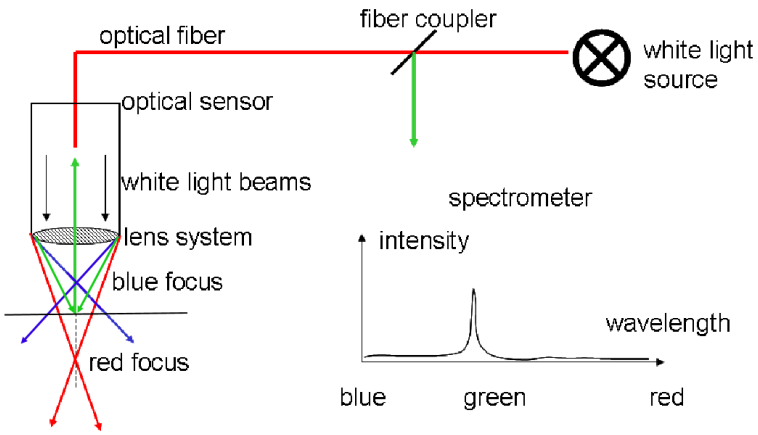

2. Chromatic topography sensor [16].

Stripe projection

Another common surface measurement technique also applied to paper is stripe projection. We used a GFM Micro CAD instrument, like the one described by Frankowski and Hainich [17]. The basic idea of the measurement technique is shown in **Fig. 3**. A sequence of different stripe patterns is projected to the object surface and the distorted reflection pattern is imaged by a camera. Knowing the geometry of the setup, the shape of the object can then be reconstructed. This makes use of both triangulation and the phase information of the projected stripe patterns. The instrument is rather fast because it does not contain moving mechanical parts.

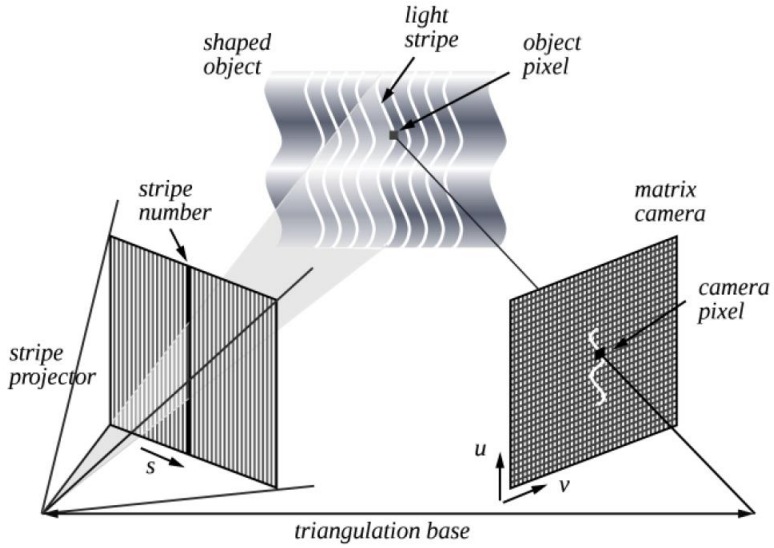

3. Surface topography measurement using stripe projection [17].

Laser profilometry

Laser profilometry, described for instance in [9], is a combination of optical and mechanical components, as depicted in **Fig. 4**. In this study we have used a UBM / Lehmann laser profilometer. A laser light spot is projected on a surface and the reflected light is imaged on an array of photodiodes. The size of the laser spot projected on the surface depends on the position of the objective lens; the size is at minimum when the objective is in focal position. The reflecting image of the laser spot is analyzed at the photodiode array and the focal position of the objective lens is adjusted by auto-focus control until the spot is in focus. Reading out the position of the objective lens in focus directly relates

to the distance of the surface. Again, for point-wise measurement of 2D regions, the sensor head must be moved in x- and y-direction. Laser profilometry is slower than the other techniques described here, because it requires mechanical adjustment of the focus for each measurement point.

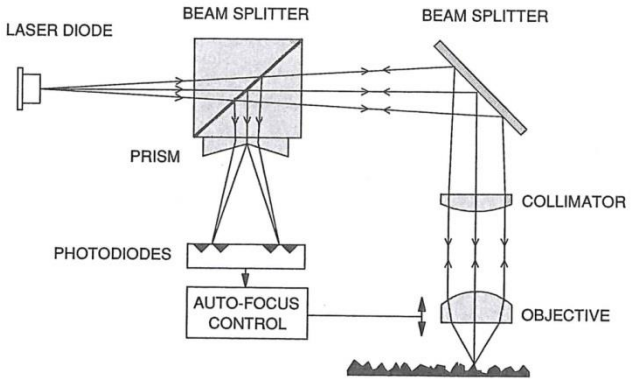

4. Laser profilometry [9].

Photometric stereo

Photometric stereo is a fast non-contact method for acquiring surface gradients [18], from which a topography map can be estimated by integration. Two or more images of the sample are first taken with a camera that is situated right on top of the sample, i.e., at viewing direction of 0º, see **Fig. 5**. For each image, the sample is illuminated from a different tilt angle (τ), keeping the slant angle (σ) constant. The choice of the slant angle should depend on the roughness of the sample [19]. Large slant angles highlight the surface shape but may also cause the surface peaks to cast shadows which are not desired. The inference of the surface orientation (i.e., gradients) from the intensity images relies on the assumption that the intensity in a point depends directly on the gradient coordinates at that point, given the additional assumptions about imaging geometry and surface reflection model. A Lambertian reflection model is typically assumed in case of paper samples due to its simplicity, although paper surface does not exactly follow the Lambertian behavior in micrometer scale. Problems caused by specular reflections can be alleviated by using crossed polarizers [20]. Once the surface gradients have been estimated, the surface topography is computed from the gradients by integration that involves noise removal and compensation of the point spread function.We use an integration method similar to that described by Hansson and Johansson [20] for estimating paper surface topography maps.

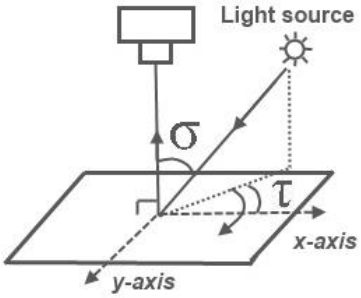

5. Measurement principle for photometric stereo [10].

The illumination in our photometric stereo arrangement was implemented by white led lights situated at tilt angles 0º, 90º, 180º and 270º, and slant angle 75º. We used crossed polarizers to eliminate the specular reflections, as in [20]: the illumination was polarized parallel to the plane of incidence (i.e., p-polarized), and the polarizer in front of the objective lens of the camera was such that only perpendicular polarized (i.e., s-polarized) light was detected.

Sample material and testing procedure

In order to compare the topography measurement systems, we analyzed five commercial paper grades, all produced on industrial paper machines. The papers covered a large range of smoothness, two coated and three uncoated, as follows:

1. Woodfree coated paper (WFC), glossy, basis weight 90 g/m², PPS 10 roughness 0.7 µm.
2. Supercalendered paper (SC-A), basis weight 65 g/m², PPS roughness 1.2 µm.
3. Lightweight coated paper (LWC), glossy, basis weight 60 g/m², PPS roughness 1.8 µm.
4. Office paper, basis weight 80 g/m², PPS roughness 4.5 µm
5. Kraft sack paper, basis weight 120 g/m², PPS roughness 7.7 µm

Each sample was marked with holes using a laser to identify a 20 mm by 20 mm measurement region [21]. The hole pattern, exemplified in **Fig. 6**, is asymmetric in order to provide unambiguous information about the sample position from the measurement result. Surface topography, including the holes, was measured with the five topography measurement techniques described above. Two specimens from each paper grade were measured. The pixels were square in each measurement technique, and the pixel sizes were as follows: 6.4 µm in shape-from-focus, 10 µm for chromatic sensor, 22.6 µm in stripe projection, 12.5 µm in laser profilometry, and 7.3 µm in photometric stereo.

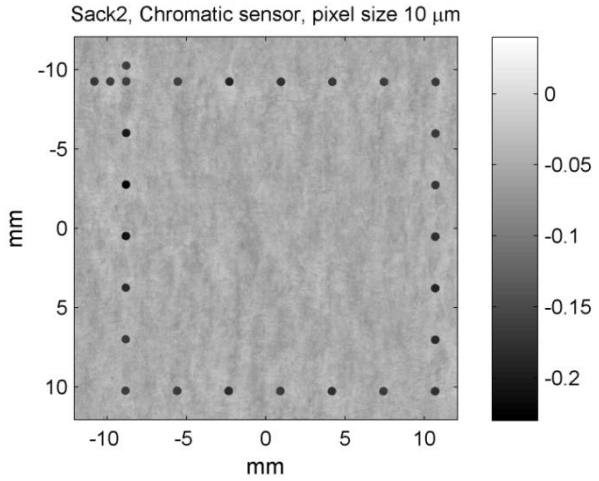

6. A sack paper paper sample with laser hole marks. The colorbar unit is also millimeter.

Analysis of similarity between the measurements

The analysis of the measurement data consists of the following actions: preprocessing, image registration and alignment, band-pass filtering, and the evaluation of the similarities between the measurements. These steps will be described in the following.

The preprocessing of the topography maps first removed spurious surface height readings from the original data by thresholding. A maximum of 0.1 % of the brightest and darkest intensity values in the image data (i.e., highest and lowest surface height values) were cut out. Some measurements, particularly from laser profilometer, contained patterns of clearly erroneous measurement values, such as high-contrast streaks. They were detected and marked as invalid analysis area. A second order polynomial fit was then removed from each topography map to correct tilt and potential curvature of the paper sample. The polynomial was fitted to the height values, excluding the hole pattern.

The images were registered using the stripe projection measurement as a reference, because it had the lowest spatial resolution. The automatic search procedure detected approximately 300 matching point pairs from the pair of images, using cross-correlation as a similarity measure between the surroundings

of the points. In some cases, we manually indicated parts of the hole pattern (Fig. 6) from the image pair to start off the automatic point search algorithm, if the texture in the topography maps did not seem similar enough. Affine transformation was fitted to the matching point pairs by a least squares method. After registration, the stripe projection measurement was upsampled to the resolution of the laser profilometer, 80 pixels per millimeter, and all the topography maps were warped by their affine transformations and interpolated to match the reference map in this resolution.

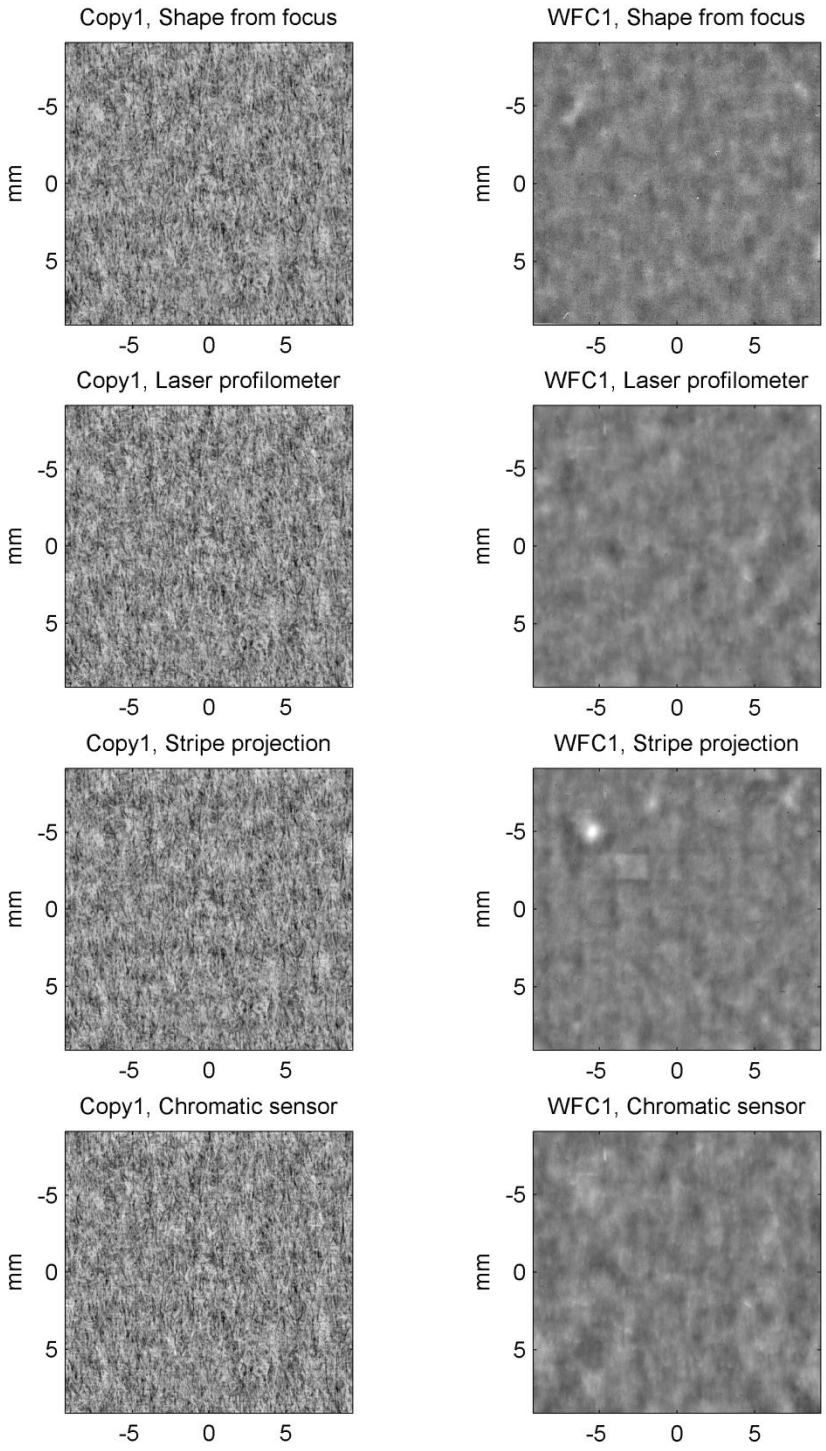

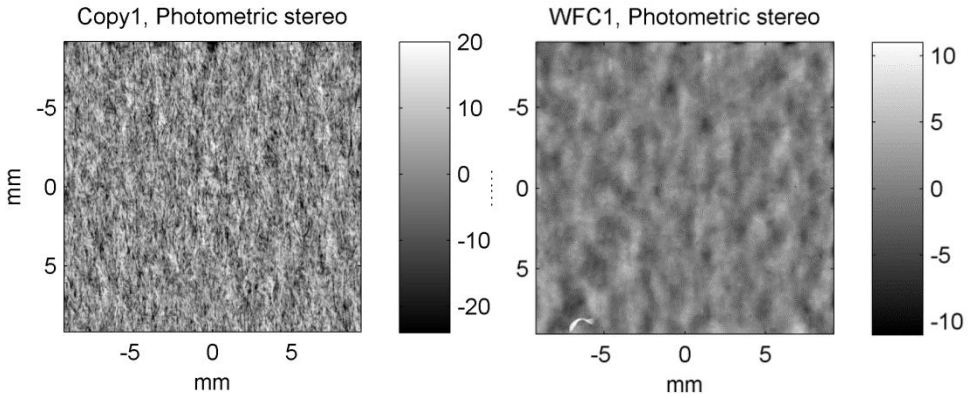

7. Aligned surface topography maps of copy and WFC papers. Wavelengths longer than 3.2 mm have been removed. The unit of the colorbars is µm.

Next we inspected the aligned image stack and its local correlations visually to assess the success of the aligment. A temporary removal of wavelengths longer than 3.2 mm revealed plenty of details from the topography and typically improved the pair-wise correlations between images. Registration and alignment was performed again for an image pair if it improved the pair-wise correlations in the whole stack of images. The final aligned image series are shown in **Fig. 7** for two paper samples, copy (office) and WFC. In copy paper, the different measurement techniques produce very similar topography maps, but in the smoothest grade tested, the images are not so similar although they all present exactly the same region of the WFC sample.

Finally, we band-pass filtered the aligned topography maps with various wavelength limits to analyze the similarity between the measurements at specified structure size ranges. The shorter wavelength limit of the chosen passband (i.e., the low-pass) was achieved by low-pass filtering the image in spatial domain with a small Gaussian kernel. The longer wavelength limit (i.e., the high-pass) was realized in two steps: first a low-pass filtering with larger wavelength, and then the subtraction of the low-pass filtered image from the original image. All the high-pass filters applied in this work follow this principle.

We chose two size ranges to quantify the similarity between the measurements. The small size range covers structures with wavelength from 25 µm to 300 µm. This range was chosen because the variance covered in this range correlates well with traditional air leakage based roughness measurements like Parker Print Surf (PPS) [22]. The larger size range covers the wavelengths from 100 µm to 3000 µm, a range that has been found to be the most important for print quality [23]. The size ranges were implemented by band-pass filtering the topography maps prior to analyses, as described above. For comparison, the results were also computed on a band from 100 µm to 20 mm which is the longest wavelength possible in these images.

The similarity between the measurements was quantified in three ways. First, we evaluated the pair-wise correlations between the aligned surface topography maps for each specimen. Both the small and large size ranges were examined, using a set of discretized bandpass limits. Second, we quantified by the coefficient of determination, how large portion of a chosen measurement's variance can be explained by the other four measurements through multivariate linear regression. The regression analysis was only performed in the large size range. Third, we compared the S_q roughness indices computed from the surface topography maps in the small size range. All the images were cropped so that the edges and the hole pattern were left out of the analysis area. This resulted in a total of 2.1 million multivariate data points for each specimen, which provides a solid base for statistical analyses.

RESULTS AND DISCUSSION

We first computed the Pearson correlation coefficients of local height coordinates from pairs of surface topography maps. **Tables I-V** present the squared correlation coefficients (R^2) at the wavelength bands 100...3000 µm and 25...300 µm. Each entry is the average value from two specimens of the same paper grade, with one exception: One of the two chromatic sensor measurements of copy paper turned out to be unusable, and therefore the entries in the third column and fourth row of Table II are based on only one copy paper sample.

	Laser profilometer	**Stripe projection**	**Chromatic sensor**	**Photometric stereo**	**Laser profilometer**	**Stripe projection**	**Chromatic sensor**	**Photometric stereo**
Shape from focus	0.38	0.69	0.79	0.74	0.21	0.51	0.63	0.41
Laser profilometer		0.34	0.42	0.38		0.19	0.22	0.18
Stripe projection			0.62	0.76			0.51	0.35
Chromatic sensor				0.73				0.31

I. Sack paper. R^2 between surface topography maps, averaged over two paper samples. Wavelengths 100...3000 µm on the left, and wavelengths 25...300 µm on the right half of the table.

	Laser profilometer	**Stripe projection**	**Chromatic sensor**	**Photometric stereo**	**Laser profilometer**	**Stripe projection**	**Chromatic sensor**	**Photometric stereo**
Shape from focus	0.90	0.87	0.93	0.82	0.68	0.69	0.83	0.72
Laser profilometer		0.85	0.93	0.84		0.71	0.82	0.70
Stripe projection			0.90	0.78			0.77	0.71
Chromatic sensor				0.43				0.38

II. Copy paper. R^2 between surface topography maps, averaged over two paper samples (except chromatic sensor, only one paper sample). Wavelengths 100...3000 µm on the left, and wavelengths 25...300 µm on the right half of the table.

	Laser profilometer	**Stripe projection**	**Chromatic sensor**	**Photometric stereo**	**Laser profilometer**	**Stripe projection**	**Chromatic sensor**	**Photometric stereo**
Shape from focus	0.26	0.21	0.13	0.07	0.01	0.02	0.01	0.04
Laser profilometer		0.32	0.38	0.25		0.16	0.39	0.25

Stripe projection			0.16	0.11			0.16	0.22
Chromatic sensor				0.56				0.18

III. SCA paper. R^2 between surface topography maps, averaged over two paper samples. Wavelengths 100...3000 µm on the left, and wavelengths 25...300 µm on the right half of the table.

	Laser profilometer	**Stripe projection**	**Chromatic sensor**	**Photometric stereo**	**Laser profilometer**	**Stripe projection**	**Chromatic sensor**	**Photometric stereo**
Shape from focus	0.25	0.25	0.21	0.03	0.02	0.01	0.02	0.01
Laser profilometer		0.50	0.58	0.16		0.31	0.60	0.40
Stripe projection			0.43	0.07			0.33	0.36
Chromatic sensor				0.39				0.49

IV. LWC paper. R^2 between surface topography maps, averaged over two paper samples. Wavelengths 100...3000 µm on the left, and wavelengths 25...300 µm on the right half of the table.

	Laser profilometer	**Stripe projection**	**Chromatic sensor**	**Photometric stereo**	**Laser profilometer**	**Stripe projection**	**Chromatic sensor**	**Photometric stereo**
Shape from focus	0.18	0.17	0.09	0.06	0.00	0.01	0.00	0.00
Laser profilometer		0.21	0.30	0.23		0.05	0.18	0.09
Stripe projection			0.13	0.09			0.03	0.06
Chromatic sensor				0.53				0.10

V. WFC paper. R^2 between surface topography maps, averaged over two paper samples. Wavelengths 100...3000 µm on the left, and wavelengths 25...300 µm on the right half of the table.

The results show that, when tested on copy paper, the five measurement devices capture very similar topography maps. Correlations between the topography maps are also quite high in case of sack paper, particularly on the larger size range. The lower R^2 values of the laser profilometer measurements for this paper are related to measurement problems with sample 1; for sample 2 the R^2 values are in the range of the other measurement techniques. For smoother papers, especially WFC (Table V), the correlations are weak. The 100-3000 µm wavelength band yields higher correlations than the 25-300 µm band in almost every pair-wise comparison. This is mainly due to random noise that weakens the signal-to-noise ratio of the measurements at high frequencies. As an exception, the photometric stereo based topography maps from LWC, and partly SC, correlate better with the others when the wavelength range is limited to the small size range. This may be related to the fact noted by previous authors, e.g., Spence and Chantler [19], that the large shapes of the surface can be inaccurate in the photometric stereo based estimate, because the surface gradients must be integrated to obtain height

data. More experiments should, however, be made to understand why this does not occur on all paper grades.

Figure 8 shows the squared correlation coefficients (R^2 values) averaged from the squared pair-wise correlation coefficients. In contrast to the results shown in Tables I-V, Fig. 8 presents only the larger size range (100-3000 µm wavelength band). The topography data has been low-pass filtered to remove wavelengths shorter than 100 µm, and then high-pass filtered to keep only wavelengths from 100 µm to the upper limit given by the abscissa. The curves represent averages from two specimens of the same paper grade, with an exception in the chromatic sensor measurements of copy paper, as noted above.

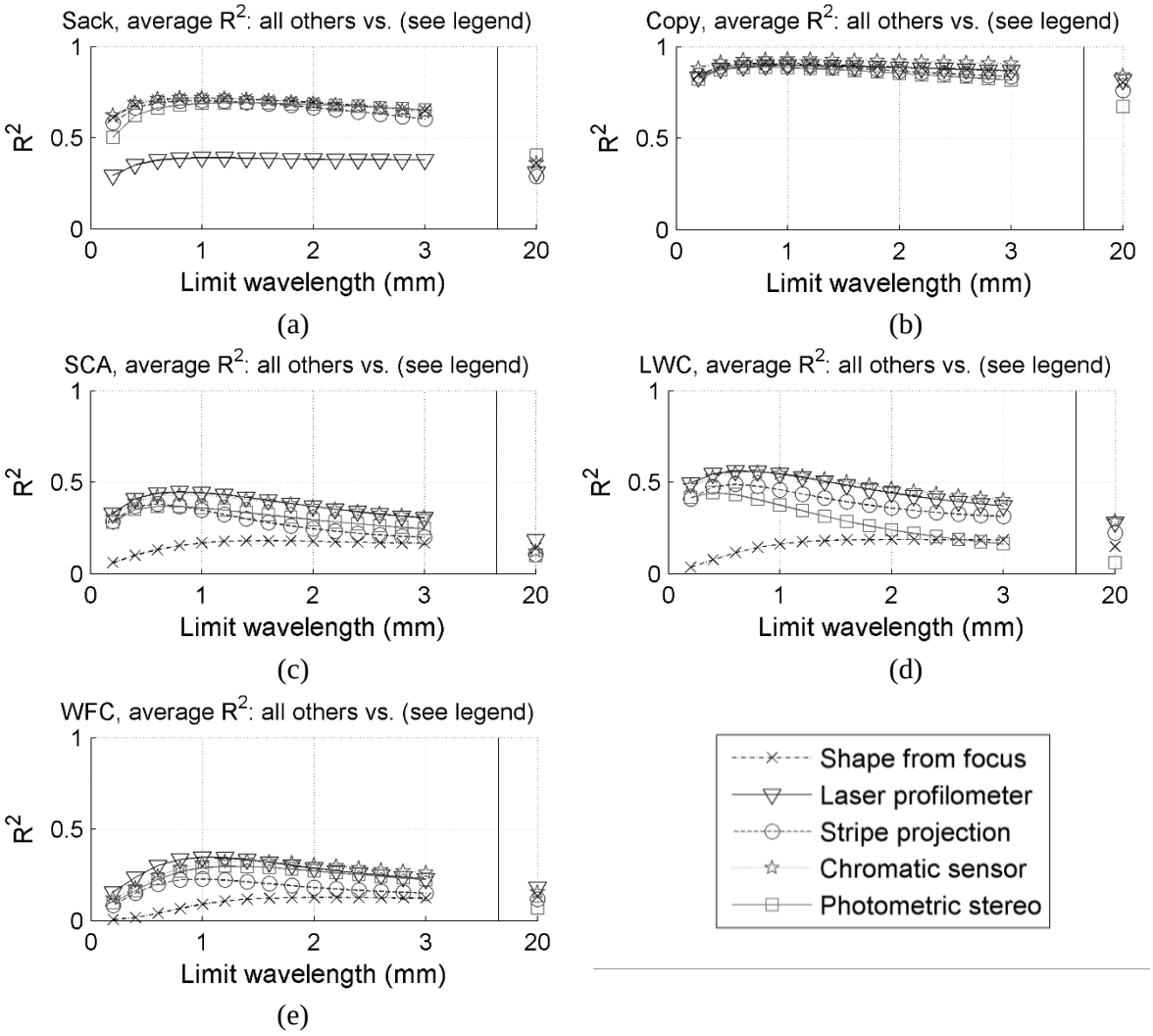

8. Averaged squared correlation coefficients. The pair-wise R^2 values were computed between a chosen measurement (see the legend box in the lower right segment) and the other four measurements, and these R^2 values were averaged. The results are shown as a function of high-pass filtering limit wavelength for paper grades from Sack to WFC in subplots (a)-(e). The low-pass limit wavelength was 100 µm.

The averaged R^2 values as a function of the long wavelength limit of the passband look quite similar to each other in the smooth paper grades (SCA, LWC, WFC). The rougher papers, Copy and Sack, form another "subgroup" of similar behavior. It seems typical in this data set that the averaged correlation gets its maximum in the band from 100 µm to approximately 1 mm. The coefficient of determination is the lowest in WFC which is the smoothest grade evaluated in this work. However, the R^2 values do not show a completely consistent increase towards the roughest paper. Thus there are other reasons for

the differences between the topography maps obtained by the various devices. Apart from the discrepancy caused by the Sack specimen 1, the laser profilometer measurement shows the strongest correlations with the other measurements. SFF seems to have its own way of measuring smooth paper grades; it produces the least similar topography maps compared to the other devices.

Figure 9 presents the results from regression analysis, in which one measurement was being explained by the other four through a multivariate linear regression model. The regression analysis was limited to the larger size range (100-3000 µm wavelength band).

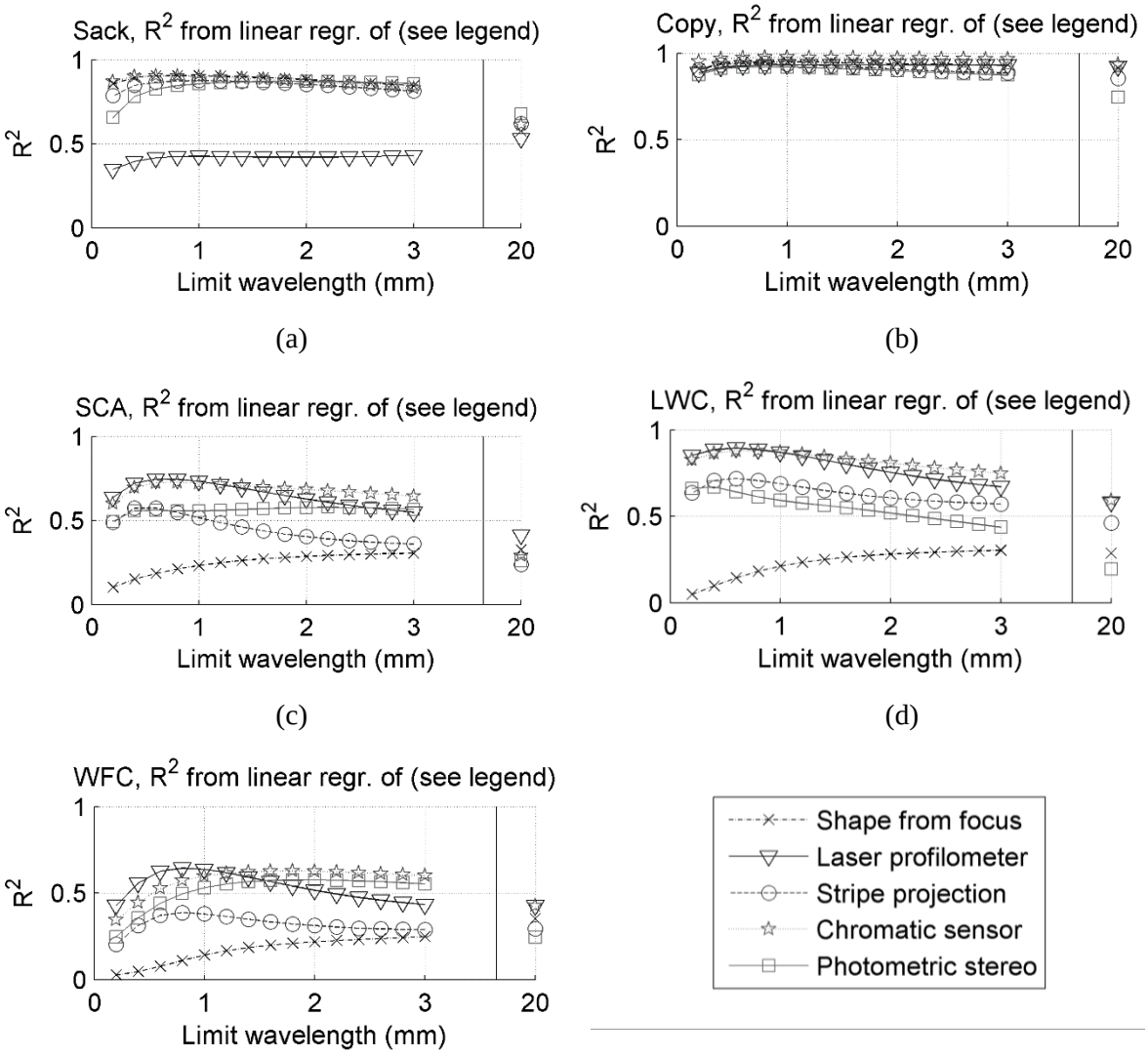

9. Coefficients of determination from multivariate linear regression in which the measurement indicated by the legend box (in the lower right segment) was being explained by the other four measurements. The results are shown as a function of high-pass filtering limit wavelength for paper grades from Sack to WFC in subplots (a)-(e). The low-pass limit wavelength was 100 µm.

The R^2 values in the regression analysis are higher than in the previous presentation that only averaged the pairwise correlation coefficients. The results have particularly improved in the smooth grades. The wavelength band in which the R^2 is maximized is similar to that found in the previous analysis; including wavelengths longer than approximately 1 mm does not usually improve the coefficient of determination. The results shown in Figs. 8 and 9 thus indicate that, apart from the SFF measurement, on a limited size range, a topography map can usually be pretty well explained by the linear combination of the other maps, even though the pair-wise correlation between a chosen pair of

measurements may not be particularly strong. This reveals that the different measurement techniques capture *systematically* different parts of the topography information.

Our third way of quantifying the differences and similarities between the surface topography measurement techniques is to compare the roughness indices computed from the topography maps. The roughness index S_q was evaluated from each topography map in the small size range (band limits from 25 µm to 300 µm) which should correspond the size range captured by air leakage based roughness measurements [22]. The correlation coefficient between the average S_q values and the PPS roughness indices of the samples is high, $R^2 = 0.97$ ($p = 0.0028$). The S_q results are presented in **Fig. 10** on a logarithmic scale to emphasize the differences between the measurement methods.

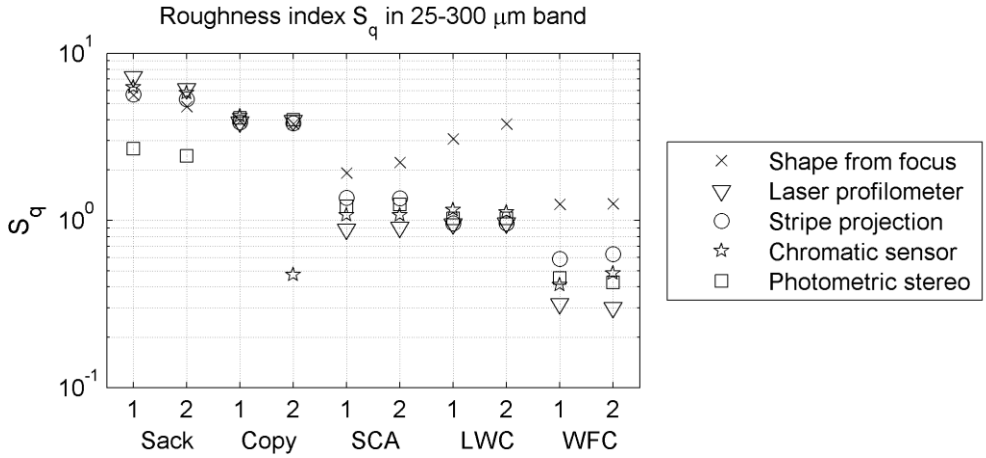

10. Roughness indices from each specimen and each measurement. Paper grade and specimen number are indicated on the x-axis.

Figure 10 clearly indicates the main deficiencies of the measurements. The photometric stereo method produces surface topography estimates that do not sufficiently capture the small-scale roughness from rough papers. The shape from focus technique exaggerates the small-scale roughness in the smoother grades (SCA, LWC, WFC). The laser profilometer gives systematically lower roughness indices from smooth grades than the other devices. Figure 10 also reveals the faulty chromatic sensor measurements of copy paper specimen 2. For comparison, we computed the S_q values in the large size scale (100 µm...3000 µm) as well, but the results are not shown here to save space. The large scale roughness results largely confirmed the findings reported above. The photometric stereo method was found to underestimate the roughness of sack paper and overestimate it in the other grades. The most notable difference between the small and large size range examination was that, in the large size range, the SFF based topography maps gave similar S_q indices as laser profilometer, stripe projection and chromatic sensor throughout the range of paper grades. This, together with the other results presented in this work, implies that the SFF measurements of smooth papers are largely governed by noise at short wavelengths (< 1 mm).

CONCLUSIONS

For rougher grades like sack paper or office paper the topography measurements from the five measurement techniques investigated showed corresponding results. For a moderately smooth LWC paper (PPS roughness 1.8 µm) the measured topographies agreed to some degree and for smooth SC and WFC papers the agreement was poor. It can be concluded that for rougher paper representative results can be obtained with all five techniques investigated. For smooth papers the measured surface topography largely depends on the applied measurement technique, and the results differ from each other notably.

There is a strong general trend that the measurements agree better with increased roughness. However, the material on the surface – fibers, fillers, bleached or unbleached pulp – is also playing a role, but not as large as the paper roughness. For all paper grades the measurement results showed better agreement for larger structures in the topography (wavelength 0.1 - 3 mm) than for small structures (0.025 - 0.3 mm).

From the available data it is impossible to tell which of the measurement techniques delivers the true surface topography of smooth papers, if any. The RMS roughness values S_q deviated considerably for some techniques also supporting the conclusion that the investigated techniques are not able to correctly capture the true surface topography and roughness. Linear modeling revealed that the differences for the smoother papers are not only due to noise but have systematic character, most likely the different measurement principles exhibit characteristic systematic errors. Further work should be aimed to find a method to measure the true paper surface topography and subsequently evaluate the correctness of the optical techniques.

ACKNOWLEDGEMENT

The authors would like to acknowledge Elmar Wind (TU Graz) for the measurements with the GFM Micro CAD and UBM Lehmann instruments and Christina Westerlind (SCA R&D Centre, Sundsvall) for the measurements with the FRT instrument. The funding from the Academy of Finland (Dec. No. 258124) is also gratefully acknowledged.

LITERATURE CITED

1. Barros, G. G. and Johansson, P.-Å., *Nordic Pulp Paper Res. J.* 21(2): 172(2006).
2. Feirer, V., Friedl H., and Hirn, U., *J. Applied Statistics* 40(3): 626(2012).
3. Mettänen, M., Hirn, U., Lauri, M., et al., *14th Fund. Res. Symp.*, 2009, FRC, Lancashire, p. 1293.
4. Dunfield, L. G, McDonald, J. D., Gratton, M. F., et al., *J. Pulp Paper Sci.* 12(2): 31(1986).
5. Quintana, E., Gomez, N., and Villar, J. C., *Appita J*. 65(3): 262(2012).
6. Kasajova, M. and Gigac, J., *Nordic Pulp Paper Res. J.* 28(3): 443(2013).
7. Cruz, M. A., Joyce, M., Fleming, P. D., et al., *2007 Papermakers Conference*, TAPPI, p. 11.
8. Wågberg, P. and Johansson, P.-Å., *Tappi J.* 76(12): 115(1993).
9. Mattsson, L. and Wågberg, P., *Precision Eng.* 15(3): 141(1993).
10. Kuparinen, T., "Reconstruction and analysis of surface variation using photometric stereo", Ph.D. thesis, Lappeenranta University of Technology, Lappeenranta, Finland, 2008.
11. Mettänen, M., Jukola, M., Miettinen, A., et al., *2011 Progress in Paper Physics Seminar*, TAPPI, p. 225.
12. Lechthaler, M. and Bauer, W., *Wochenblatt für Papierfabrikation* 134(21): 1227(2006).
13. Lähdekorpi, M., Ihalainen, H., and Ritala, R., *XVIII IMEKO World Congress*, 2006, IMEKO, Budapest.
14. Danzl, R., Helmli, F., and Scherer, S., *Strojniski vestnik-J. Mech. Eng*. 57(3): 245(2011).

15. Scherer, S., Danzl, R., Heimli, F., et al., *Wochenblatt für Papierfabrikation* 135(21-22): 1192(2007).

16. Fries, T., *2009 IEEE Advanced Semiconductor Manufacturing Conference*, IEEE / SEMI, p. 184.

17. Frankowski, G. and Hainich, R., *SPIE Photonics West - Emerging Digital Micromirror Device Based Systems and Applications III*, 2011, SPIE, Vol. 7932, Article number 79320D.

18. Woodham, R. J., *Optical Eng.* 19(1): 139(1980).

19. Spence, A. D. and Chantler, M. J., *IEE Vision, Image and Signal Processing* 153(2): 149(2006).

20. Hansson, P. and Johansson, P.-Å., *Optical Eng.* 39(9): 2555(2000).

21. Hirn, U., Kritzinger, J., Donoser, M., et al., *14th Fund. Res. Symp.*, 2009, FRC, Lancashire, p. 721.

22. Chinga, G., Johnsen, P. O., Dougherty, R., et al., *J. Microscopy* 227(3): 254(2007).

23. Feirer, V., Hirn, U., Friedl, H., et al., *Advances in Printing and Media Technology XXXVIII*, 2011, IARIGAI, p. 93.